Variability and Trends in the Southern Hemisphere High Latitude, Quasi-Stationary Planetary Waves

John Turner, J. Scott Hosking, Thomas J. Bracegirdle, Tony Phillips and Gareth J. Marshall

British Antarctic Survey, Natural Environment Research Council, High Cross,

Madingley Road, Cambridge, CB3 0ET, UK

Corresponding author address. Prof. J. Turner, British Antarctic Survey, Natural Environment Research Council, High Cross, Madingley Road, Cambridge, CB3 0ET, UK.

Tel +44 (01223) 221485, Fax +44 (01223) 221279, Email JTU@BAS.AC.UK

Running head – Southern Hem

Keywords – Antarctica; teleconnections; Southern Ocean; atmospheric circulation

Abstract

We investigate variability and trends of the Southern Hemisphere quasi-stationary planetary waves over 1979 – 2013 using the ECMWF Interim reanalyses. The effects of tropical and extra-tropical forcing factors on the phase and amplitude of the planetary waves are identified. The amplitudes of wave numbers 1-3 exhibit an annual cycle with a minimum in summer and maximum over the extended austral winter period. The phase of wave number 1 has a semi-annual cycle, moving east in austral spring/fall and west in summer/winter as a result of differences in the phase of the semi-annual oscillation across the Pacific sector of the Southern Ocean. The phase of wave number 3 has an annual cycle, being more eastward (westward) in summer (winter). Year-to-year variability of the amplitude of wave number 1 is found to be strongly associated with the Amundsen Sea Low, which in turn is known to be strongly influenced by ENSO, with the consequence that the amplitude of wave number 1 is larger during the El Niño phase of the cycle. Regarding trends for the year as a whole, the amplitude of wave number 1 has decreased since 1979 ($p < 0.1$), while the amplitudes of wave numbers 2 and 3 have increased. These changes are consistent with the warming trends in SSTs across much of the tropical oceans. However, the factors associated with longer-term trends are less clear than for year-to-year variability.

1. Introduction

In the Southern Hemisphere, the quasi-stationary planetary waves have a significant influence on a number of aspects of the climate of high southern latitudes. Analyses of the mean Southern Hemisphere geopotential height fields in the troposphere have shown that planetary wave number 1 has the largest mean amplitude of any of the quasi-stationary waves (van Loon and Jenne, 1972; Trenberth, 1980; Hobbs and Raphael, 2007), with the wave having an amplitude that is comparable to that of wave number 1 in the Northern Hemisphere. Changes in the phase and amplitude of the wave influence high pressure blocking episodes over the Southern Ocean (Renwick, 2005), sea ice distribution (Raphael, 2007; Irving and Simmonds, 2015) and regional temperatures (van Loon and Williams, 1976).

Wave number 3 has a smaller mean amplitude than wave number 1 and explains less of the tropospheric atmospheric circulation spatial variability than wave number 1 (8% compared to 90% at 60° S (Raphael, 2004)). However, the wave has been linked to blocking over the Southern Ocean (Trenberth and Mo, 1985), sea ice extent (Raphael, 2007) and the climatological Amundsen Sea Low (ASL) (Baines and Fraedrich, 1989; Raphael *et al.*, 2016), which plays an important part in controlling climate variability between the Antarctic Peninsula and the Ross Sea (Hosking *et al.*, 2013) (locations referred to in the text are shown on Figure 1). Wave number 2 is comparable to wave number 3 in amplitude for much of the year, but has the largest interannual variability of any of the planetary waves (van Loon, 1979) and is most important over the Antarctic (Trenberth, 1980).

Earlier studies have linked variability in wave number 1 to sea surface temperatures (SSTs) in the tropics and particularly the phase of the El Niño-Southern Oscillation (ENSO) (Hobbs and Raphael, 2007). A number of investigations have found strong evidence for a

Rossby Wave source in the tropical Pacific Ocean and the dispersion of a signal of ENSO to the high latitude areas of the Southern Hemisphere (Garreaud and Battisti, 1999; Renwick and Revell, 1999; Harangozo, 2000; Houseago-Stokes and McGregor, 2000; Yuan, 2004; Liu and Alexander, 2007; Jin and Kirtman, 2009; Jin and Kirtman, 2010). Hoskins and Karoly (1981) showed that areas of deep convection close to the Equator could generate Rossby waves through the vorticity created by diabatic heating. The Rossby waves were found to propagate polewards in both hemispheres and provide a means for the establishment of teleconnections between ENSO and the climates of the extra-tropical areas. This wave train was shown to be well established during the Southern Hemisphere winter in the upper air geopotential height fields during the El Niño phase (Karoly, 1989; Kiladis and Mo, 1998). The wave train from the central Pacific is known as the Pacific South American 1 (PSA-1) connection (Mo and Higgins, 1998). This was originally investigated using EOF analysis, although recently a new method for identifying and quantifying the wave train has been developed based on Fourier analysis (Irving and Simmonds, 2016)The wave train consists of an arc of high–low–high geopotential height anomalies extending in a southeastward direction towards the Antarctic from the area of increased convective activity in the central Pacific (Kidson, 1999; Yuan, 2004). The wave train affects the synoptic conditions across the southern part of South America, as well as the Antarctic coastal region (where it also affects the sea ice distribution) between the Antarctic Peninsula and the Ross Sea, with a reduction in cyclonic activity/greater blocking to the west of the Peninsula during El Niño events (Turner, 2004; Pezza *et al.*, 2012). The area between the Antarctic Peninsula and the Ross Sea is where the ASL is located, which is broadly coincident with the climatological ridge of wave number 1 and one of the wave number 3 troughs. A wave train from the tropical Pacific Ocean that gives more or less cyclonic activity in this area therefore has the potential to affect the amplitude and phase of these waves.

Although ENSO dominates tropical variability and its high-latitude responses on timescales of a few years, longer time-scale observed multi-decadal trends show strong warming over the tropical Atlantic in recent decades. The latest research indicates that this Atlantic warming is large enough to produce a Rossby wave-related deepening of the ASL of a similar magnitude to that generated by trends in the tropical Pacific (Simpkins et al., 2014; Li et al., 2015). One common theme across these different linkages is they strongly affect the ASL region, as is seen in the year-to-year teleconnection patterns to the tropical Pacific.

The primary mode of climate variability at high southern latitudes is the Southern Annular Mode (SAM), which has an impact on the strength of the westerly winds over the Southern Ocean. Climate variability around the Antarctic is therefore affected by both tropical variability and factors at high southern latitudes that influence the phase of the SAM. In the following we will therefore consider how both these factors influence the planetary waves.

In this paper we examine the variability and change in the amplitude and phase of the quasi-stationary planetary waves in high southern latitudes. We investigate the tropical and high latitude forcing factors that have influenced the waves over recent decades. We consider wave numbers 1 to 4 as these have a much larger amplitude than the shorter waves and have been shown to have a major influence on the climate of the Antarctic (Raphael, 2007).

In Section 2 we describe the atmospheric reanalysis fields that were used and the creation of the climatology of the Southern Hemisphere planetary waves. Section 3 considers the mean amplitudes and phases of the planetary waves and their variability over the year. The factors that result in changes in the amplitude and phase of the planetary waves are examined in Section 4. The trends in the planetary waves since 1979 are discussed in

Section 5. Section 6 considers the effects of changes in the planetary waves on the climate of the Antarctic. We conclude with a discussion in Section 7.

2. Data and methods

The climatology of the quasi-stationary planetary waves was developed from the monthly mean upper air geopotential height fields from the ECMWF Interim Reanalysis (ERA-Interim) project (Dee *et al.*, 2011) covering the period 1979 - 2013. The geopotential height fields have a horizontal resolution of 0.7° × 0.7°. We have used the ERA-Interim reanalysis fields rather than other reanalysis data sets since it has been shown that the data are the most reliable when compared to Antarctic in-situ observations (Bracegirdle and Marshall, 2012). For the computation of correlations the time series of planetary wave amplitudes and phases, and the atmospheric and SST fields were all detrended. In the production of the annual mean SST correlation plots we have taken account of autocorrelation at all lags.

The amplitudes and phases of wave numbers 1 to 4 were determined by carrying out a Fourier analysis of the monthly mean 500 hPa geopotential height fields. The amplitudes of the planetary waves have a large meridional variability (Figure 2), with the largest amplitude of wave number 2 (wave numbers 1, 3 and 4) being at high (mid) latitudes. In order to minimize the noise in the time series of amplitudes and phases we have carried out the Fourier Analysis on the mean 500 hPa heights across the latitude band 55° – 65° S. This zone is largely over the Southern Ocean where the longest waves have a large amplitude and where the variability of synoptic activity has a large impact on the climate of the Antarctic continent (Turner et al., 1996). The amplitudes and phases of the longest waves were also computed for latitude bands that extended Equatorwards as far as 40° S in order to see how the results presented below would change. Even over the extended range of 40° – 65° S, wave number 1 still had the largest annual mean amplitude. However, when more northerly latitudes were included the correlations between the amplitudes of the waves and tropical Pacific SSTs decreased and were less significant.The amplitude (half the difference in geopotential height (gpm) between the ridge and trough) and phase (zonal location of the first ridge in degrees east of Greenwich) were obtained for each month allowing the investigation of changes during the annual cycle. The UK Hadley Centre's HadISST data set (http://www.metoffice.gov.uk/hadobs/hadisst/) was used to examine ocean conditions over the period. Fields of mean SIC, computed using the Bootstrap version 2 algorithm were obtained on a 25 km resolution grid from the US National Snow and Ice Data Center (http://www.nsidc.org).

3. The mean amplitudes and phases of the quasi-stationary planetary waves

The annual cycles of the amplitudes and phases of wave numbers 1 to 4 over 55-65° S in the 500 hPa geopotential height fields for the period 1979-2013 are shown in Figure 3, with annual and seasonal means being presented in Table 1. Throughout the year wave number 1 has the largest amplitude of any of the planetary waves, with the annual mean amplitudes of wave numbers 1 to 4 being 83.3, 39.8, 42.1 and 17.6 m respectively. The amplitude of wave number 1 has an annual cycle and varied from a minimum of 59.7 m in November to a maximum of 107.2 in September (Figure 3a). Wave number 1 is influenced by SSTs across the tropical and mid-latitude areas of the Pacific Ocean (Hobbs and Raphael, 2007) and the form of the annual cycle of the amplitude shown in Figure 3 is inversely related to the broadscale temperatures across the Southern Hemisphere during the year. The SSTs across the tropical oceans vary little over the year, but the amplitude of wave number 1 is largest in September when the sea ice is at its greatest extent and surface temperatures are lowest in the sea ice zone. The amplitude decreases rapidly in the spring when the sea ice retreats and temperatures increase across the high latitude areas of the Southern Ocean and over the Antarctic continent. The amplitude of wave number 2 also has a minimum in summer, with peaks in late fall and winter. The variability in the amplitude of wave number 3 over the year is similar in magnitude to that of wave number 2, with a minimum in the summer and maximum in the middle of winter. The amplitude of wave number 4 only has a range of 9.5 m over the year, with an annual cycle that is dominated by a decrease from May to October.

The annual mean zonal locations of the wave number 1 trough and ridge are respectively located at 53° E off Enderby Land and at 127° W at the boundary between the Amundsen and Ross Seas. The phase of wave 1 (Figure 3b) has a semi-annual cycle, with the trough/ridge being further east (west) during spring and fall (summer and winter). The wave shifts as the form of the semi-annual oscillation (SAO) in MSLP and 500 hPa geopotential height (Van den Broeke, 1998; Simmonds, 2003) varies around the continent. Between the Antarctic Peninsula and the Ross Sea the 500 hPa geopotential heights across 160 - 140° W drop more rapidly between February and May compared to those over 90 – 70° W, resulting in the ridge of wave number 1 in this sector moving towards the east over this period. Relative differences in the 500 hPa geopotential height variations between these two areas over the rest of the year account for the semi-annual cycle of the wave number 1 phase seen in Figure 3b.

The mean phase of wave number 2 varies by 29.2° over the year with the annual mean locations of the ridges being at 105° E and 75° W, and the troughs at 15° E and 165° W. The phase of wave number 3 exhibits a broadly annual cycle with the wave being more eastward in summer and shifting ~25° towards the west by mid-winter as the amplitude of the wave increases. Baines and Fraedrich (1989) suggested that the marked wave number 3 pattern in the Southern Hemisphere high latitude tropospheric flow is present because of the shape of the Antarctic ice sheet and the strong westerly winds over the Southern Ocean. In addition, they linked the presence of the ASL, which is coincident with one of the wave number 3 troughs, to the atmospheric flow off Victoria Land in East Antarctica. On the other hand wave number 4 exhibits no clear pattern of variability over the year.

4. Variability of the planetary waves

The planetary waves show a large inter-annual variability in both amplitude and phase (Table 1). The variability in amplitude, based on the standard deviations, is greatest in winter for the three longest waves, but is largest in fall for wave number 4. In contrast, the variability of the phase is largest in spring for wave numbers 3 and 4, but greatest in fall and summer for wave numbers 1 and 2 respectively.

As wave number 1 is strongly influenced by the surface temperature gradient across the Southern Hemisphere its amplitude and phase are significantly correlated ($p < 0.05$) with SSTs across large areas of the oceans, both in the tropics and at higher latitudes. Figure 4a shows the correlation of the annual mean amplitude of wave number 1 with the annual mean SSTs. The largest areas of significant correlation are across the tropical Pacific with a couplet of significant positive (negative) correlation on the eastern (western) side of the Pacific basin. This pattern of correlation resembles the SST anomalies associated with the El Niño phase of ENSO, when higher SSTs are found between the western coast of South America and near 180°, with negative anomalies further west. However, the region of significant correlation extends in a northeastward and southeastward fashion from the central Pacific, while the El Niño positive SST anomalies lie in a more narrow band along the Equator. As shown on Figure 4a, the correlation between the wave number 1 amplitude and SSTs in the Nino 1+2 area along the coast of South America is only 0.31, which is not significant at $p < 0.05$.

Figure 4a indicates that the amplitude of wave number 1 is larger during the El Niño phase of the ENSO cycle compared to La Niña. This is consistent with the establishment of a Rossby wave train between the central Pacific and the Amundsen-Bellingshausen Sea (ABS) during the El Niño phase, which was noted by Yuan (2004). Such a wave train has a positive geopotential height anomaly in the ABS, as illustrated in Figure 5, which shows the differences in 500 hPa geopotential height between the austral winters when ENSO was in the El Niño and La Niña phases. We focus on the winter season since this is when the tropical – high southern latitude teleconnection is most established (Trenberth *et al.*, 2014). Such a positive geopotential height anomaly will reinforce the ridge of wave number 1, which is located to the west of the Antarctic Peninsula.

The largest positive correlations in Figure 4a are across 140-180° W, which encompasses part of the Niño 3.4 area. Not surprisingly, the annual mean amplitude of wave number 1 has a correlation of 0.55 with the Niño 3.4 index. The correlations for the other three waves are all less than 0.15. A further area of significant ($p < 0.05$) positive correlation is found in the Antarctic coastal region across 100° W – 160° E, which is the location of the wave number 1 ridge throughout the course of the year (Fig. 3b). There is also an area of anticorrelation between wave number 1 amplitude and SSTs in the tropical Atlantic Ocean. This is consistent with the Rossby Wave train from this area noted by Li et al. (2014), which propagates towards the ABS, indicating that a positive SST anomaly in the tropical Atlantic would reduce the amplitude of the wave number 1 ridge located in this area.

The seasonal fields of correlation between the wave number 1 amplitude and the SSTs (not shown) are broadly similar to the annual field in Figure 4a, however, there are some differences. The winter and spring patterns of correlation are very similar to those in Figure 4a, with the correlation values being higher during the spring. This is consistent with the strong links between tropical SSTs and the warming of West Antarctica identified by Schneider et al. (2012). In summer and fall the largest correlations are further to the east, with the highest values overall being during the summer. However, in both these seasons the correlations are smaller in the Nino 1+2 area that further west, and are only significant at $p < 0.05$ during the summer.

The pattern of correlation of annual mean SST with the annual mean phase of wave 1 (Figure 4b) has some similarities to that found for the amplitude, with significant ($p < 0.05$) correlations (anti-correlations) over the eastern (western) Pacific Ocean. However, the areas where the correlations are significant are much smaller and the region of significant positive correlation is close to the coast of Peru. The correlations with SST are weaker than for the wave number 1 amplitude, possibly as a result of the wave being tied to the orography of the Antarctic, although model experiments would need to be carried out to confirm this. As with the amplitude, the pattern is similar to the SST anomalies associated with ‘classical’ ENSO events and indicates the impact that ENSO has on the phase of wave 1. However, overall the SST changes have more of an impact on the amplitude of wave number 1 than the phase. The wave is more east (west) during the El Niño (La Niña) phase because of the higher (lower) pressure over the ABS as a result of the Rossby wave train from the tropics.

For the year as a whole the amplitude of wave number 2 is not significantly ($p < 0.05$) correlated with SSTs across the bulk of the Pacific Ocean, with only small areas of the Maritime Continent having a significant correlation. In addition, there are only small areas of the South Pacific where the annual mean phase of wave number 2 is significantly correlated with SSTs.

The influences on wave number 3 are quite different to those of the longer waves. There are no significant correlations between either the wave number 3 amplitude or phase with SSTs in the tropics or extra-tropical latitudes. Rather its variability is correlated significantly ($p < 0.05$) with the zonal winds over the Southern Ocean. Figure 6a shows the correlation of the annual mean amplitude of wave number 3 and the annual mean 500 hPa zonal wind component. Care must be taken when interpreting these figures as the statistics on amplitude and phase of the planetary waves are computed from the geopotential height fields over 55° – 65° S, which are related to the winds in these latitudes through geostrophy. Nevertheless, a larger amplitude is found when the winds are stronger above the circumpolar trough around the coast of East Antarctica. In addition, the couplets of southward positive/northward negative correlation close to 90° E and 130° W indicate that a larger amplitude is found when there is a southward displacement of the mid-tropospheric jet. This is consistent with the work of Baines and Fraedrich (1989) who suggested that the wave number 3 pattern was associated with the zonal winds just north of the Antarctic coast. The seasonal correlation fields for fall, winter and spring are similar to Figure 6a, with a larger amplitude of wave number 3 associated with stronger winds just north of the Antarctic coast. However, the correlation between wave number 3 amplitude and the zonal wind is rather different in summer, with the highest correlations being across 30-50° S. The amplitude of the wave is at a minimum at this time of year (Fig. 3a), as is the speed of the westerly winds, and the wave is clearly more influenced by conditions outside of the Antarctic.

The phase of wave number 3 is also correlated significantly with the speed of the winds over the southern ocean (Figure 6b) and the areas of significant correlation are larger than for the amplitude, indicating that changes in the zonal wind speed have a stronger relationship with the phase of wave number 3 than the amplitude. The couplet of negative/positive correlation across the Southern Ocean indicates a strong association between a southward displacement of the mid-tropospheric jet and a more eastward location of the wave.

Tropical SST variability has little impact on the annual mean amplitude of wave number 4, with only SSTs across the Maritime Continent having slightly stronger, but not significant correlations (Figure 7a). Here higher SSTs, such as found during La Niña events, give a reduction in the amplitude of wave number 4. On the other hand, there is a significant anti-correlation between the amplitude of wave number 4 and SSTs to the southeast of New Zealand.

The phase of wave number 4 is influenced to a small extent by tropical SSTs with the correlation field (Figure 7b) showing some significant ($p < 0.05$) anti-correlations across the eastern Pacific, although the correlations are low. During strong El Niño events, with higher SSTs off tropical South America there will be greater blocking in the Bellingshausen Sea and a westward displacement of wave number 4. An assessment of the differences in MSLP between years of large and small wave number 4 amplitude shows that the largest differences are over the Amundsen-Bellingshausen Sea, although the differences are not significant at $p < 0.05$.

5. Trends in the amplitude and phase of the planetary waves

The greatest changes in the planetary waves since 1979 have been with wave number 1, which has decreased in amplitude throughout the year, with the trend for the year as a whole being significant at $p < 0.10$ (Table 2a). In contrast, the annual mean amplitudes of waves 2 and 3 have increased, although it should be noted that neither of the trends are significant. Since 1979 there has been a significant ($p < 0.05$) warming across the Maritime Continent, in the mid-latitude areas of the North and South Pacific, and in the tropical and northern mid-latitude areas of the Atlantic (Figure 8). According to recent modelling studies, for the period 1979-2009 positive SST trends across much of the tropical ocean areas induced a deepening of the ASL in spring, along with pressure increases off East Antarctica that are consistent with a weakening of wave number 1 (Simpkins *et al.*, 2014). The pattern of SST trends shown in Figure 8 is found in all four seasons, with the magnitudes of the trends also being similar throughout the year. The Simpkins et al. (2014) findings are likely to vary across the annual cycle, but the link between tropical Atlantic warming and ASL deepening appears from modelling studies to also be important in winter (Li *et al.*, 2015). The smallest trend in the wave number 1 amplitude is in the summer when the tropical – high latitude teleconnections are weakest. The largest trend is in the winter when the teleconnection is most established. The enhanced cyclonic circulation in the region of the ASL (Turner *et al.*, 2016) reduces the amplitude of wave number 1 since this is the location of the climatological wave number 1 ridge.

The two largest seasonal trends in wave number 3 amplitude have occurred in summer and fall, although the signs of the trends are different. In summer the climatological mid-tropospheric jet is located over the Southern Ocean close to 45° S and the amplitude of wave number 3 is anti-correlated with the wind speed at this latitude and positively correlated with the wind speed further south. Since the early 1980s the depletion of stratospheric ozone has had a profound impact on the atmospheric circulation of high southern latitudes (Thompson *et al.*, 2011). Although the loss of stratospheric ozone has been greatest during the spring, the impact in the troposphere is largest during the summer. One consequence has been to play a major part in the trend of the SAM moving into its positive phase, although the phase of the SAM is also affected by SSTs in the tropical Pacific (Ding *et al.*, 2012). The SAM is the primary mode of atmospheric variability at high southern latitudes and when in its positive phase the winds over the Southern Ocean are stronger. Since the late 1970s there has been a strengthening and southward shift in the Southern Hemisphere jet during the summer giving a couplet of stronger (weaker) winds further south (north). Although the SAM is essentially an annular mode, the loss of stratospheric ozone has also given a decrease in MSLP in the ABS (Fogt and Zbacnik, 2014) where one of the wave number 3 troughs is climatologically located, so the 'ozone hole' will have contributed to an increase in the amplitude of wave number 3 during the summer, although other factors will have played a part.

Around much of the Antarctic in the fall the mid-tropospheric jet is located just close to 50° S, with the strongest winds north of East Antarctica. However, in the South Pacific sector there is a well developed split jet (Bals-Elsholz *et al.*, 2001), with the two branches located near 30° (the sub-tropical jet) and 60° S (the polar front jet) to the north and south of New Zealand. During the fall the amplitude of wave number 3 is significantly correlated with the zonal wind above the circumpolar trough around the coast of East Antarctica, north of the Weddell Sea and across the Antarctic Peninsula into the Bellingshausen sea (Fig. 6a). During the fall there has been a significant (p < 0.05) weakening of the zonal wind above the circumpolar trough north of East Antarctica and the Bellingshausen Sea, with the amplitude of wave number 3 having decreased by 2.61 m dec^{-1}, although this trend is not significant.

The trends in the annual mean phases of wave numbers 1, 3 and 4 are rather small and none of the trends are significant. However, wave number 2 has experienced a larger eastward annual mean shift of over 4° dec^{-1} since 1979, although the trend is still not significant because of the large inter-annual variability and the near-zero trend in winter. The positive trend of SSTs since 1979 in the tropical oceans (Figure 8) has contributed to lower MSLP and geopotential heights in the ABS through the establishment of a Rossby Wave train to this region. Since the climatological location of one of the wave number 2 ridges is at 76° W, just to the east of the Antarctic Peninsula, the MSLP/geopotential height anomalies over the ABS have played a part in the eastward displacement of wave number 2.

The trends in the phase of wave number 4 are quite different in the four seasons. The largest trend, although not significant, has been in spring with an eastward shift of 2.81° dec^{-1}. This is the only season during which the phase of the wave is significantly correlated with SSTs across the tropical Pacific, with an ENSO like pattern of positive (negative) correlations over the Maritime Continent (eastern Pacific). With the observed warming across the Maritime Continent this would be consistent with an eastward shift in wave number 4. The only significant ($p < 0.10$) trend in the phase is a westward shift of 2.69° dec^{-1} during winter. The phase during this season is not correlated significantly with tropical SSTs, but is significantly correlated with SSTs across parts of the Southern Ocean. In particular, it is anticorrelated with SSTs to the southeast of Australia in an area where there has been significant warming since 1979. While change in this area is significantly correlated with the wave number 4 phase, it is likely that other factors have played a part in the observed trend.

6. The impact of changes in the planetary waves on the Antarctic climate

As noted in Section 1, changes in the phase and amplitude of the planetary waves can affect a number of aspects of the Antarctic and Southern Ocean climate system, including surface temperature, sea ice extent and climatological low pressure systems, such as the ASL. Of course variability in these quantities is interrelated since changes in atmospheric circulation will alter the wind field, which will in turn affect the thermal advection and surface temperatures, and also result in changes in the sea ice distribution, which is highly correlated with the near-surface winds (Holland and Kwok, 2012).

The sector of the Antarctic between the Antarctic Peninsula and the Ross Sea has the highest sensitivity to changes in the planetary waves since both wave numbers 1 and 2 have a climatological ridge located here, and one of the wave number 3 troughs is found close to the location of the ASL. This is also the region where the strongest teleconnections between the tropics and Antarctica are found, and as discussed previously, the tropical influences have a strong impact on the planetary waves.

Here we examine how the annual mean amplitude and phase of wave numbers 1 to 4 are related to the annual mean sea ice concentration, surface temperature and precipitation. A summary of the significant relationships is provided in Table 3.

The variability in the wave number 1 amplitude is correlated significantly with a number of key climatic elements to the west of the Antarctic Peninsula.The amplitude of wave number 1 has the largest correlation with Antarctic sea ice concentration of any of the amplitudes or phases of the four longest planetary waves. The amplitude is significantly correlated (anticorrelated) with the concentration of sea ice over the Bellingshausen-Weddell Seas (Ross Sea), indicating that a smaller amplitude is linked with less (more) sea ice along the Antarctic Peninsula (over the Ross Sea). A similar pattern of correlation is found with near-surface air temperature (Figure 9) and precipitation amount. The areas of significant positive correlation are mainly over the ocean for near-surface air temperature, but extent across much of the western part of West Antarctica with precipitation. As shown in Table 1, since 1979 the amplitude of wave number 1 has decreased, which is consistent with the greater cyclonic activity in the region of the ASL and the dipole of changes between the Antarctic Peninsula and the Ross Sea. The Antarctic Peninsula has been affected by a marked decrease in sea ice extent over the Bellingshausen Sea (Turner *et al.*, 2015), a rise in near-surface temperature (Turner *et al.*, 2005) (which is strongly linked to the loss of sea ice) and greater precipitation (Turner *et al.*, 1997). In contrast, the Ross Sea has had the largest increase in sea ice extent of any sector of the Antarctic, with the ERA Interim reanalyses suggesting a small decrease in precipitation, although there has been no significant change in temperature. The phase of wave number 1 has less of an impact on the climate of the Antarctic, but is linked to sea ice and temperature off Wilkes Land and precipitation around the tip of the Antarctic Peninsula.

The phase of wave number 2 is also important in modulating the regional climate of West Antarctica. A more eastward location of the wave is associated with less sea ice over the Bellingshausen Sea, since this is the location of one of the wave number 2 ridges, and an eastward shift would introduce more cyclonic conditions and a greater northerly flow. Such an eastward shift of the wave is also associated with higher near-surface temperatures and greater precipitation. However, the amplitude of wave number 2 has no significant impact on sea ice distribution or temperature, and only influences precipitation across small parts of West Antarctica and the Weddell Sea.

Since one of the troughs of wave number 3 is located off West Antarctica it is not surprising that changes in this planetary wave have an impact on the climate of the region. Changes in the amplitude of the wave have relatively little impact on the climate of West Antarctica, with a greater amplitude just slightly increasing the concentration of sea ice near the coast of West Antarctica and giving higher air temperatures near 180° as there is more northerly flow in this area. The greatest impact of wave number 3 variability is felt with changes in the phase. The eastward location of the wave is significantly correlated (anticorrelated) with the sea ice concentration over the Amundsen Sea (Ross Sea) as the meridional winds are altered in these areas. These sea ice anomalies correspond with near-surface air temperatures with more (less) sea ice being associated with colder (warmer) air temperatures.

The amplitude of wave number 4 is anticorrelated with sea ice extent between the Antarctic Peninsula and the Ross Sea, and correspondingly correlated with surface temperature in this region. The greatest impact of changes in phase of this wave area are felt around the Antarctic Peninsula (see Table 3).

Although the greatest effects of planetary wave variability are felt between the Antarctic Peninsula and the Ross Sea there are some statistically significant links in other parts of the Antarctic. In particular, an eastward shift in the phase of wave numbers 2 and 3 is associated with more sea ice off East Antarctica between 20° E and 50° E.

7. Discussion and conclusions

This study has documented the climatology of the amplitude and phase of the quasi-stationary planetary waves in high southern latitudes. The results indicate that tropical ocean conditions, especially across the Pacific, have a major influence on the amplitude and phase of the planetary waves at high southern latitudes, consistent with known mechanisms for tropical-Antarctic teleconnections. The greatest influence is in the sector between the Antarctic Peninsula and the Ross Sea, where wave numbers 1 and 2 both have a climatological ridge. The year-to-year variability of the waves is strongly correlated with the phase of ENSO, which has its largest influence on the three longest waves. During the El Niño phase the increased convection near 180° E generates a Rossby Wave train that extends into both hemispheres, with the impact in the Antarctic coastal zone being greatest in the ABS where the wave number 1 and 2 ridges are located. For the year as a whole, variability in the wave number 1 amplitude and wave number 2 phase has a significant impact on MSLP over the ABS, which in turn influences the sea ice extent, temperature and precipitation.

Over the reanalysis period since 1979 the SSTs across parts of the tropical oceans have increased, tending to decrease MSLP in the ASL region. This has led to a statistically significant ($p < 0.1$) decrease in the amplitude of wave number 1.

Other modes of climate variability are also related to the state of the planetary waves. As discussed earlier, changes in the SAM have varied around the continent and its zonal variability can be related the waves. The SAM is the primary mode of atmospheric variability at high southern latitudes and changes in the SAM can affect many aspects of the climate system (Thompson *et al.*, 2011). As shown earlier, wave number 3 is affected much less by tropical SSTs than the other planetary waves and its variability is more associated with the strength of the westerly winds over the Southern Ocean. These in turn are strongly influenced by the phase of the SAM so that changes in the SAM are related to the state of wave number 3.

Over the next century it is expected that the depletion of stratospheric ozone during the austral spring (the ozone hole) will recover, but it seems likely that greenhouse gas concentrations will increase. This will give a warming at the Earth's surface of several degrees, with the largest increases occurring over the land areas. A number of factors will influence how the Southern Hemisphere planetary waves will change over the coming decades (Freitas and Rao, 2014). However, a factor of particular importance to the Southern

Hemisphere planetary waves is how the ENSO cycle will change. Unfortunately, the current generation of coupled climate models give no clear indication as to how the ENSO cycle will change and whether there will be a greater frequency of El Niño or La Niña events (Vecchi and Wittenberg, 2010). Since the amplitudes and phases of the Southern Hemisphere planetary waves are strongly dependent on the phase of ENSO it is not possible at present to predict how these will change over the coming decades.

Acknowledgements

This work forms part of the British Antarctic Survey Polar Science for Planet Earth programme. It was supported by the UK Natural Environment Research Council under grant NE/K00445X/1.

Figure captions.

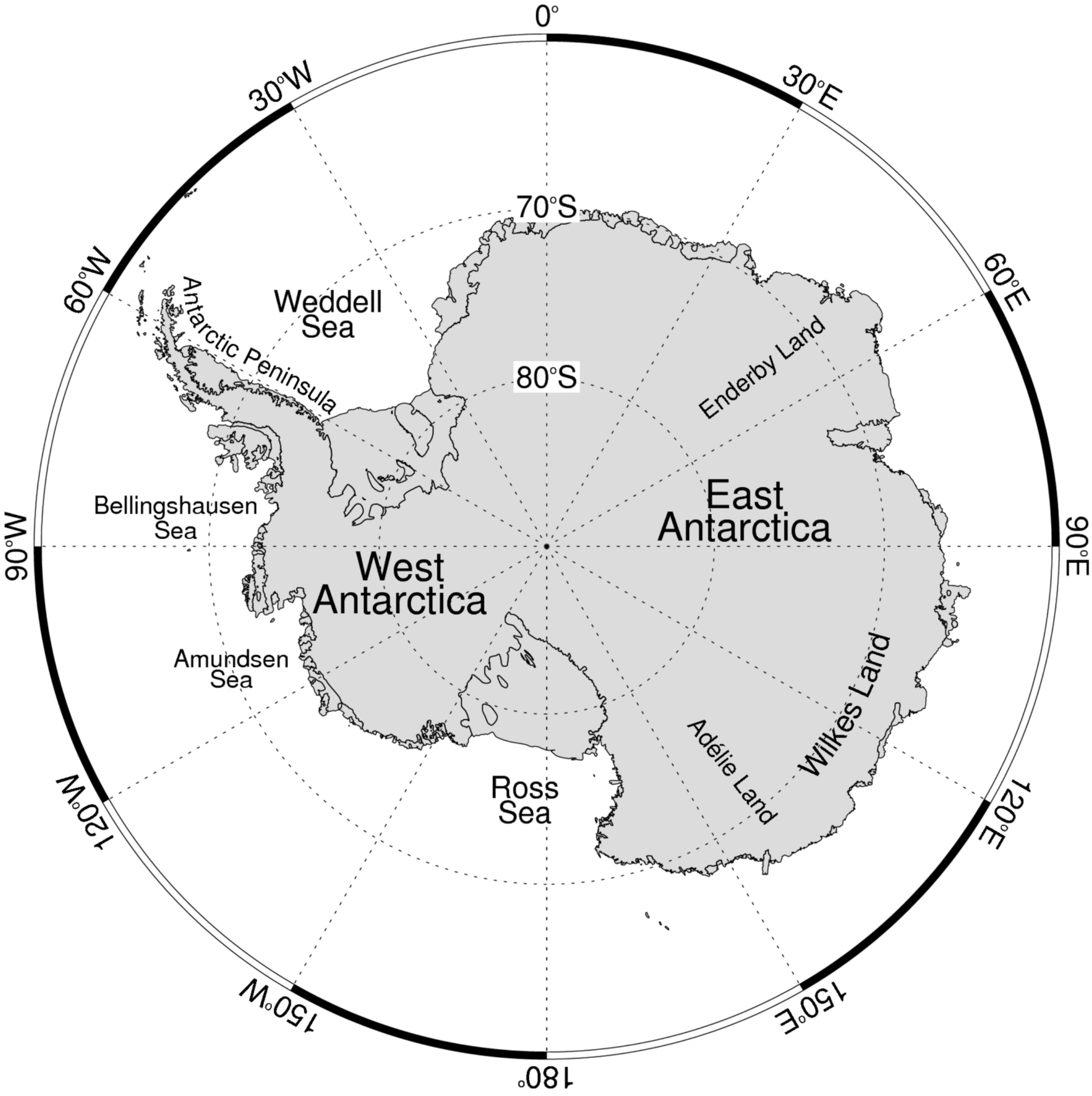

Figure 1. Map showing the locations referred to in the text.

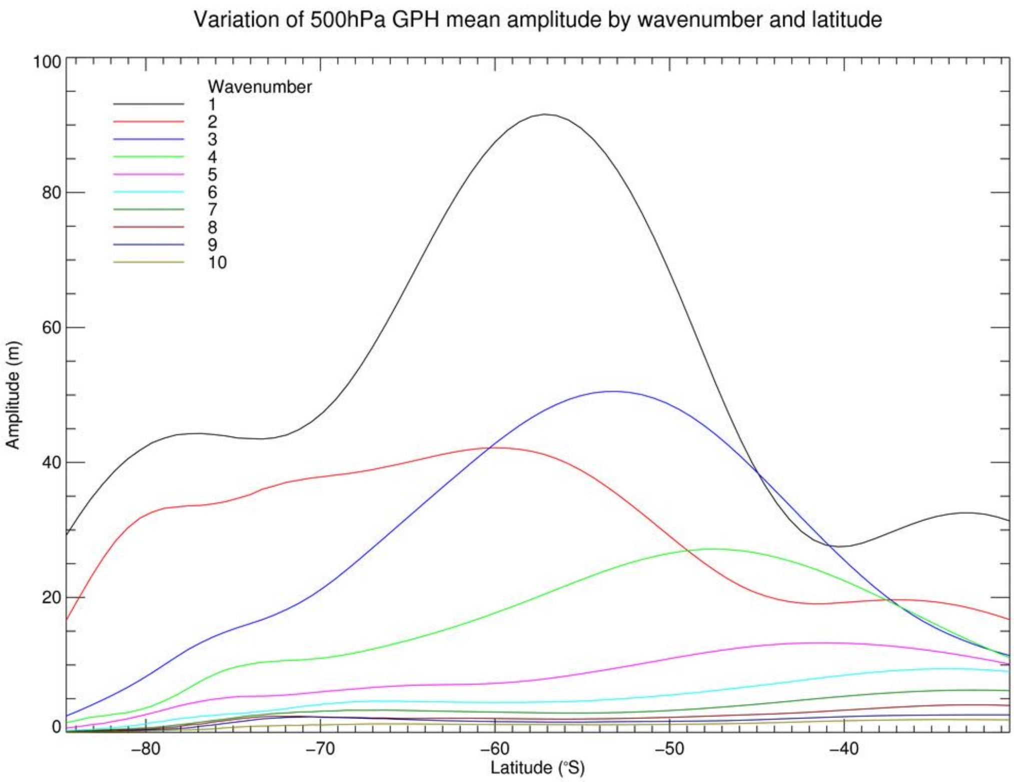

Figure 2. The zonal mean amplitudes (m) of wave numbers 1 to 10 across 30 - 90° S for 1979 - 2013.

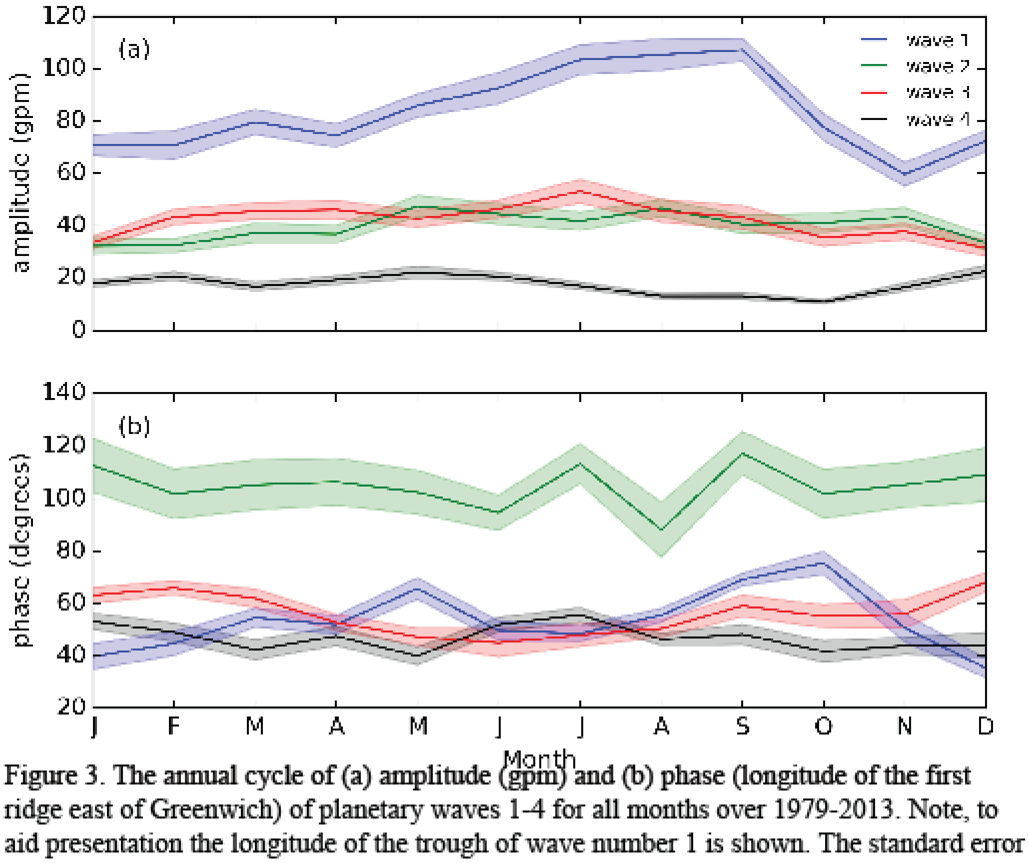

Figure 3. The annual cycle of (a) amplitude (gpm) and (b) phase (longitude of the first ridge east of Greenwich) of planetary waves 1-4 for all months over 1979-2013. Note, to aid presentation the longitude of the trough of wave number 1 is shown. The standard deviation of the mean is indicated by the shading.

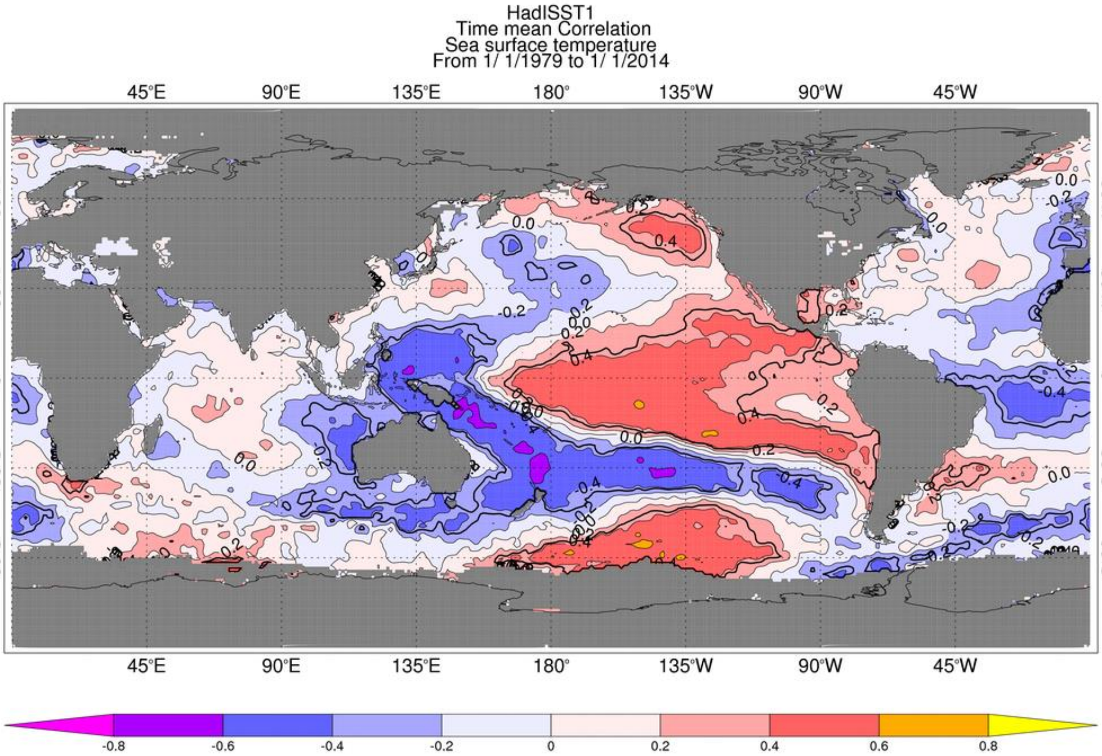

Figure 4a. The correlations of annual mean SSTs with (a) wave number 1 annual mean amplitude, (b) wave number 1 annual mean phase, (c) wave number 2 annual mean amplitude and (d) wave number 2 annual mean phase   Areas where the correlations are significant at $p < 0.05$ are enclosed by a bold line.

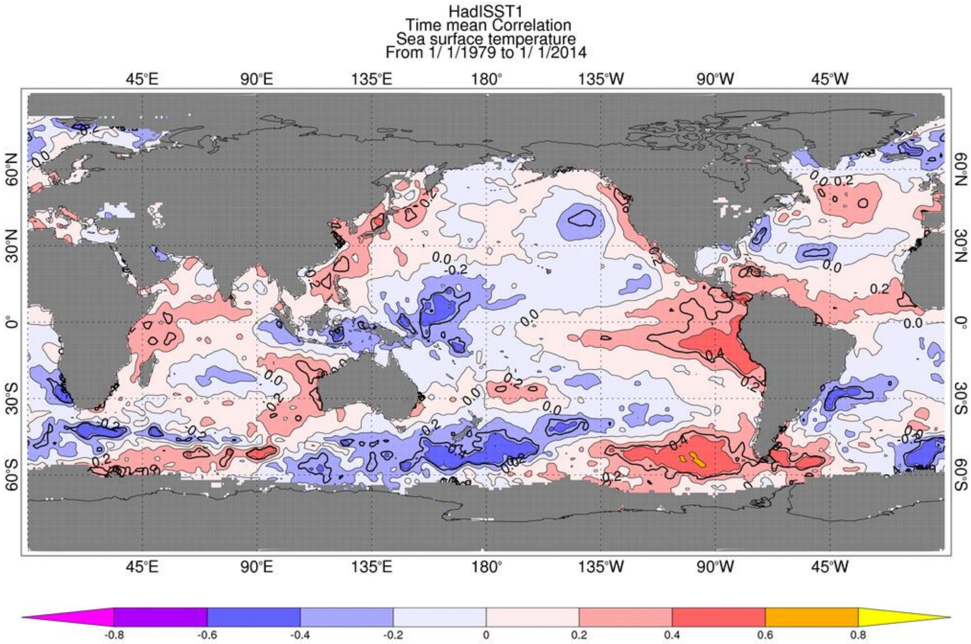
HadISST1
Time mean Correlation
Sea surface temperature
From 1/ 1/1979 to 1/ 1/2014
45°E 90°E 135°E 180° 135°W 90°W 45°W
60°N 30°N 0° 30°S 60°S
-0.8 -0.6 -0.4 -0.2 0 0.2 0.4 0.6 0.8

Figure 4b

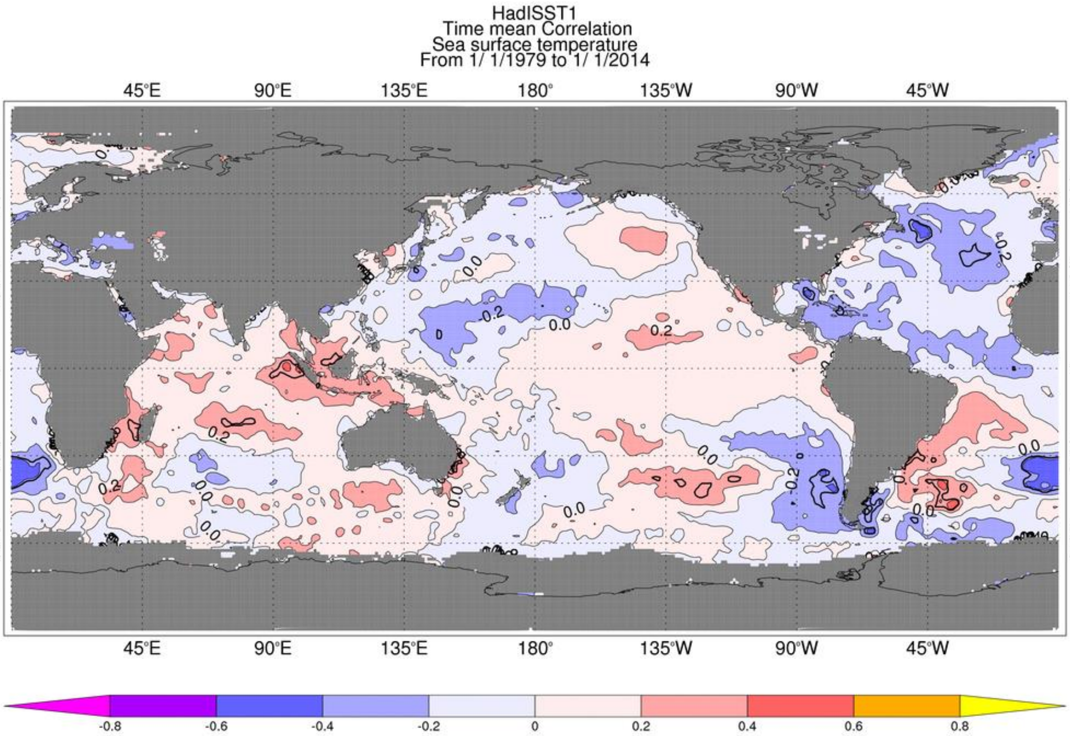

Figure 4c

497

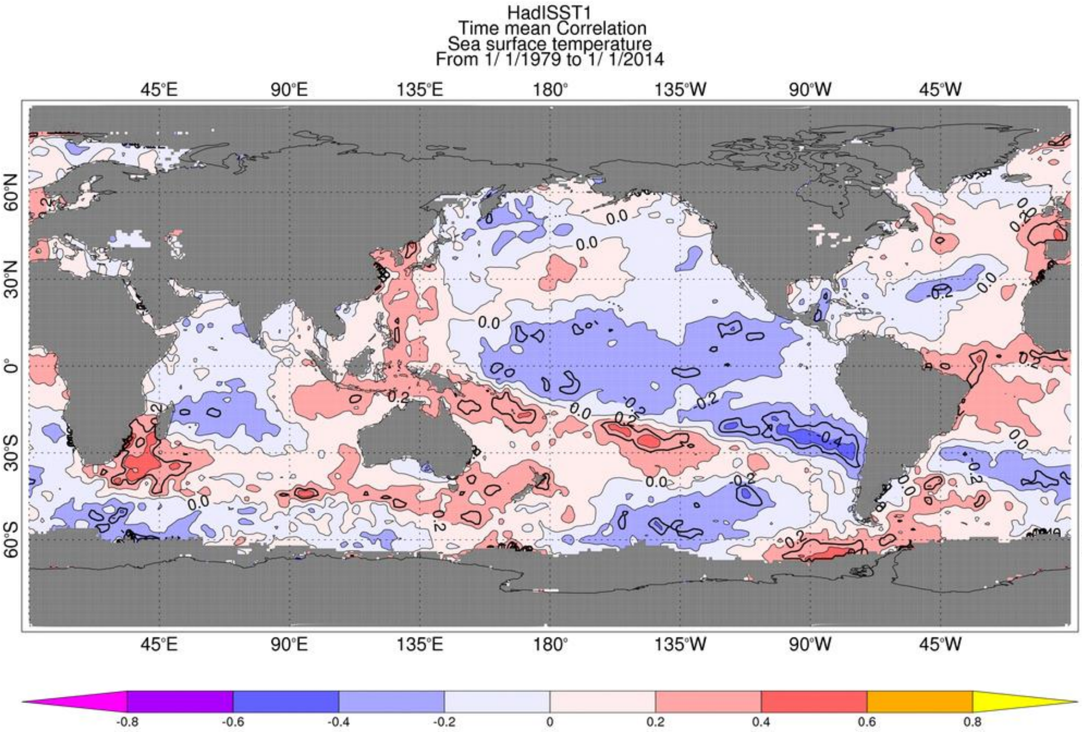

Figure 4d

Figure 4. The correlations of annual mean SSTs with (a) wave number 1 annual mean amplitude, (b) wave number 1 annual mean phase   Areas where the correlations are significant at $p < 0.05$ are enclosed by a bold line.

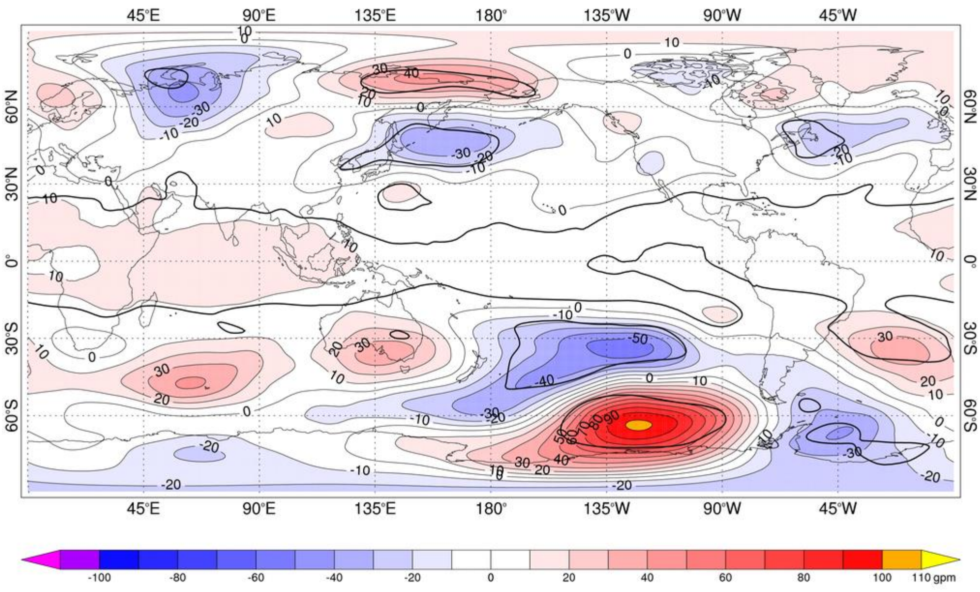

Figure 5. The differences in 500 hPa geopotential height (gpm) between the austral winters when the tropical Pacific was in the El Niño (1982, 1987, 1991, 1997, 2002) and La Niña (1981, 1984, 1985, 1988, 1989, 1999, 2000) phases of the ENSO cycle. Areas where the differences are significant at $p < 0.05$ are enclosed by a bold line.

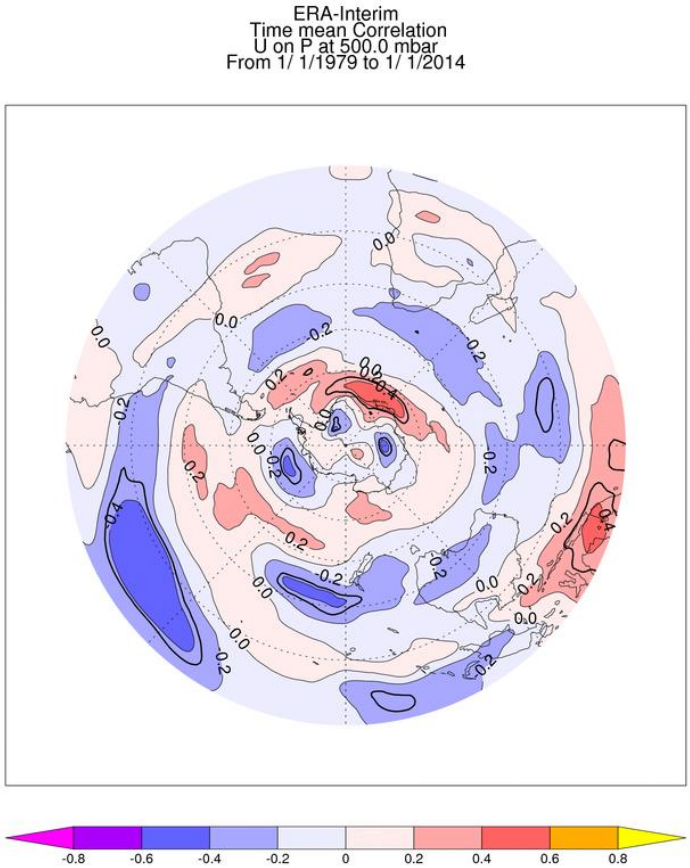

Figure 6a. The correlation of the annual mean (a) amplitude and (b) phase of wave number 3 with the annual mean zonal wind component at 500 hPa for 1979-2013. Areas where the correlations are significant at $p < 0.05$ are enclosed by a bold line.

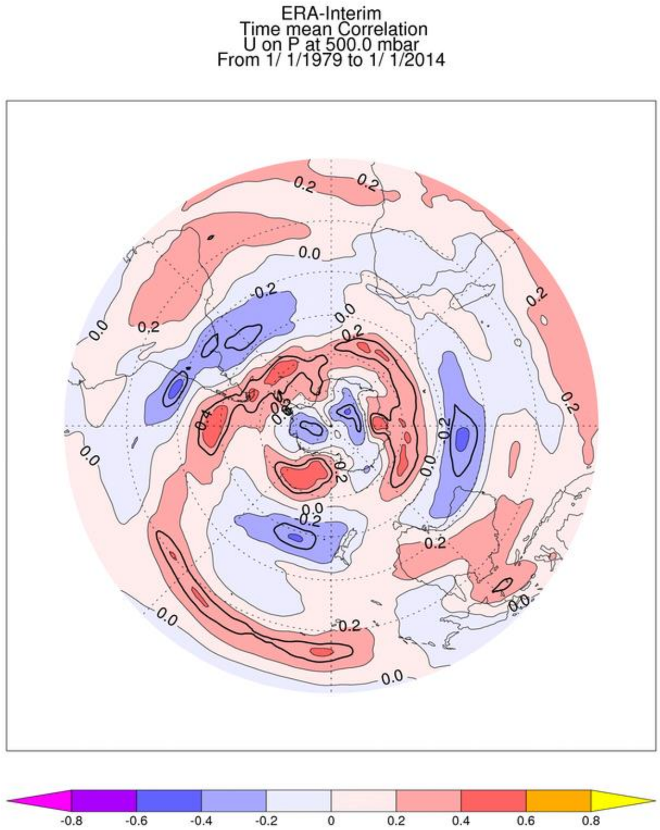

Figure 6b

Figure 6. The correlation of the annual mean (a) amplitude and (b) phase of wave number 3 with the annual mean zonal wind component at 500 hPa for 1979-2013. Areas where the correlations are significant at $p < 0.05$ are enclosed by a bold line.

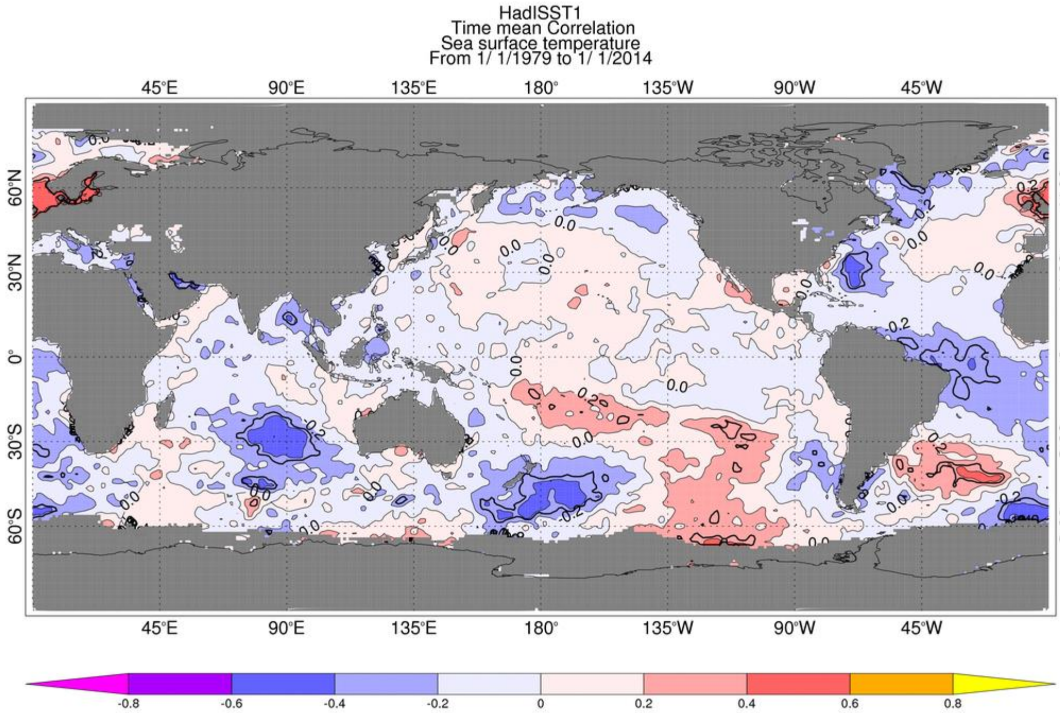

Figure 7a. Correlations of the annual mean (a) amplitude and (b) phase of wave number 4 with the annual mean SST for 1979 - 2013. Areas where the correlations are significant at $p < 0.05$ are enclosed by a bold line.

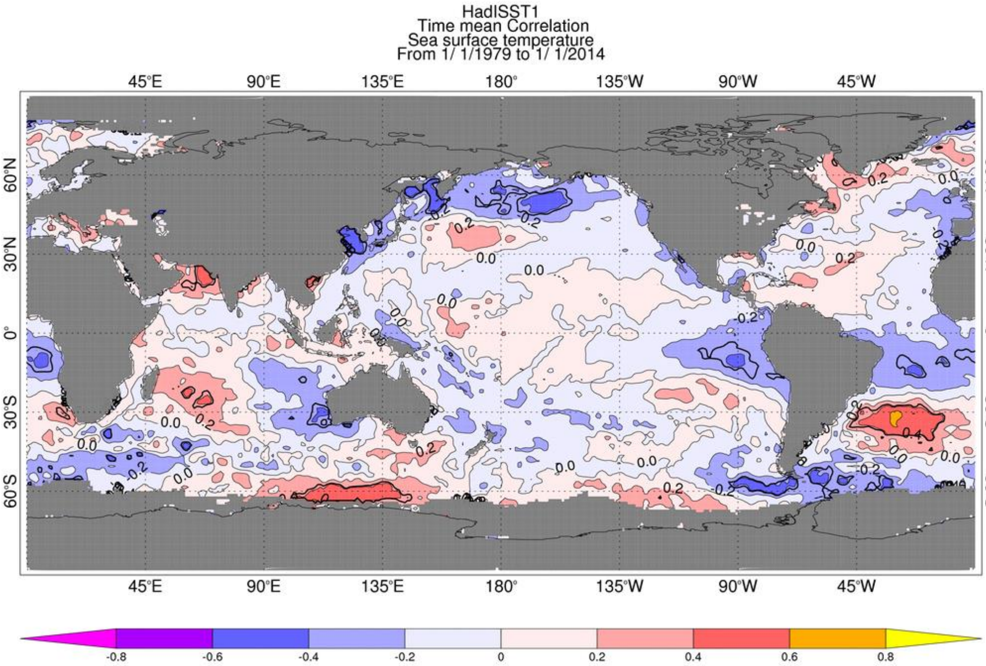

Figure 7b

Figure 7. Correlations of the annual mean (a) amplitude and (b) phase of wave number 4 with the annual mean SST for 1979 - 2013. Areas where the correlations are significant at $p < 0.05$ are enclosed by a bold line.

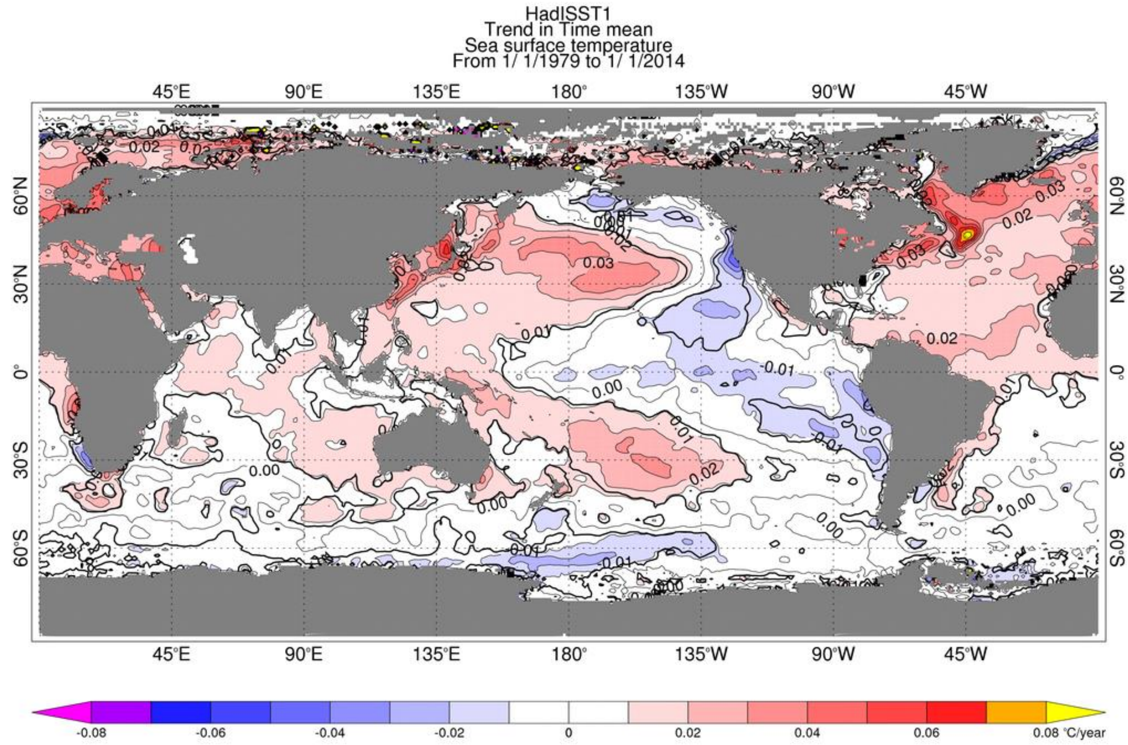

Figure 8. The trend in annual mean SST for 1979 – 2013. Areas where the trends are significant at p < 0.05 are enclosed by a bold line.

Figure 8. The trend in annual mean SST for 1979 – 2013. Areas where the trends are significant at $p < 0.05$ are enclosed by a bold line.

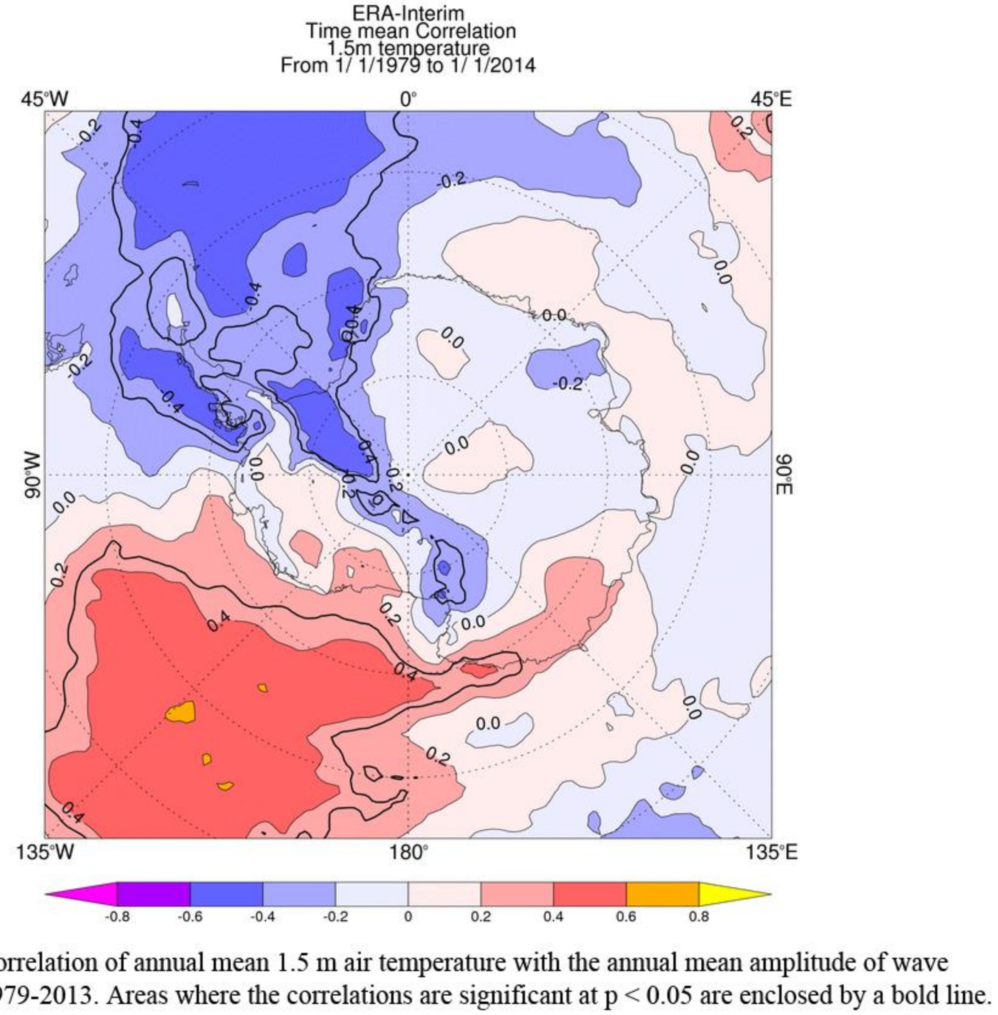

Figure 9. The correlation of annual mean 1.5 m air temperature with the annual mean amplitude of wave number 1 for 1979-2013. Areas where the correlations are significant at $p < 0.05$ are enclosed by a bold line.

Table captions

Wave number	Summer (DJF)	Fall (MAM)	Winter (JJA)	Spring (SON)	Year
1	71.4 (18.4)	80.0 (19.1)	100.5 (22.8)	81.5 (17.3)	83.3 (13.1)

2	32.9 (10.9)	40.5 (12.1)	44.4 (12.9)	41.7 (11.2)	39.8 (6.2)
3	36.3 (8.1)	44.8 (11.1)	48.4 (12.6)	38.9 (12.3)	42.1 (4.4)
4	20.6 (6.4)	19.4 (7.4)	17.0 (4.6)	13.6 (4.3)	17.6 (2.9)

Table 1a.

Wave number	Summer (DJF)	Fall (MAM)	Winter (JJA)	Spring (SON)	Year
1	140.6 W (14.9)	122.7 W (15.2)	128.8 W (10.4)	114.9 W (13.8)	126.6 W (7.3)
2	108.2 E (36.0)	104.7 E (33.6)	98.7 E (30.8)	108.1 E (32.7)	104.8 E (17.1)
3	65.6 E (11.8)	53.9 E (12.1)	47.7 E (15.6)	56.7 E (19.5)	56.0 E (7.6)
4	48.1 E (13.2)	43.2 E (13.2)	51.2 E (9.2)	44.5 E (13.4)	46.9 E (6.4)

Table 1. The zonal mean annual and seasonal (a) amplitudes (m) and (b) phases (degrees east of Greenwich of the first ridge) of wave numbers 1 to 4 over 55° – 65° S for 1979-2013. The standard deviations are given in parentheses.

Wave	Summer	Fall	Winter	Spring	Year

number					
1	-0.82 ± 6.50	-4.77 ± 6.14	-5.81 ± 7.33	-4.47 ± 5.56	-3.64* ± 4.20
2	-0.46 ± 3.83	0.75 ± 4.02	-0.35 ± 4.29	1.83 ± 3.68	0.58 ± 2.07
3	2.29 ± 2.76	-2.61 ± 3.58	-0.50 ± 4.19	1.36 ± 4.05	0.11 ± 1.48
4	-0.28 ± 2.22	-1.64 ± 2.41	-0.47 ± 1.53	1.12 ± 1.39	-0.15 ± -.96

Table 2a.

Wave number	Summer	Fall	Winter	Spring	Year
1	1.17 ± 5.16	0.62 ± 5.04	1.39 ± 3.44	2.57 ± 4.50	1.08 ± 2.39
2	4.38 ± 12.63	9.15 ± 10.76	0.82 ± 10.27	4.63 ± 10.78	4.24 ± 5.55
3	0.40 ± 4.16	0.32 ± 4.02	1.46 ± 5.17	2.81 ± 6.42	1.06 ± 2.50
4	-0.91 ± 4.39	-1.58 ±4.35	-2.69* ± 2.92	2.81 ± 4.37	-0.31 ± 2.14

Table 2b

Table 2. The zonal mean annual and seasonal trends in (a) the amplitudes (m dec^{-1}) and (b) the phases (degrees dec^{-1}) of wave numbers 1 to 4 over 55° – 65° S for 1979-2013. Significance is indicated as $p < 0.1$ (*).

Wave number	Amplitude	Phase
1	**Sea ice.** Correlated (anticorrelated) over the Bellingshausen-Weddell Seas (Ross Sea).	**Sea ice**. Correlated (anticorrelated) off Wilkes Land (West Antarctica).

	Temperature. Correlated (anticorrelated) over the Ross Sea (Bellingshausen-Weddell Seas). **Precipitation**. Correlated over western West Antarctica and the Ross Sea.	**Temperature**. Anticorrelated (correlated) off Wilkes Land (West Antarctica). **Precipitation**. Correlated (anticorrelated) in the coastal areas of West Antarctica to Victoria Land (around the tip of the AP and over Wilkes Land).
2	**Sea ice.** No links. **Temperature**. No links. **Precipitation**. Anticorrelated across small areas of West Antarctica and the Weddell Sea.	**Sea ice.** Anticorrelated (correlated) over the Bellingshausen Sea (north of Dronning Maud land). **Temperature**. Correlated (anticorrelated) from the Bellingshausen Sea to the Weddell Sea (over East Antarctica and off Dronning Maud land). **Precipitation**. Correlated (anticorrelated) over the AP and eastern West Antarctic (western West Antarctica).
3	**Sea ice.** Correlated (anticorrelated) along the coast of West Antarctica (in the Weddell Sea). **Temperature**. There is a small area of correlation over western West Antarctica. **Precipitation**. Anticorrelated (correlated) over the Amundsen Sea (small parts of East Antarctica).	**Sea ice.** Correlated (anticorrelated) over the Amundsen Sea, Weddell Sea and north of Dronning Maud land (Ross Sea). **Temperature**. Anticorrelated with temperature across West Antarctica and Dronning Maud land. **Precipitation**. Correlated (anticorrelated) across the AP (West Antarctica and Dronning Maud land).
4	**Sea ice.** Anticorrelated between the AP and Ross Sea. **Temperature**. Correlated over the	**Sea ice.** Correlated around the tip of the AP/northern Weddell Sea.

	Ross Sea and the western part of West Antarctica. **Precipitation**. Correlated over western West Antarctic and Wilkes Land (the Weddell Sea).	**Temperature**. Anticorrelated over the AP and northern Weddell Sea. **Precipitation**. Anticorrelated over the AP.

Table 3. The locations of significant ($p < 0.05$) links between the annual mean amplitude and phase of wave numbers 1 to 4 and sea ice concentration, surface temperature and precipitation. AP = Antarctic Peninsula.

Table 3. The locations of significant ($p < 0.05$) links between the annual mean amplitude and phase of wave numbers 1 to 4 and sea ice concentration, surface temperature and precipitation. AP = Antarctic Peninsula.

Acknowledgement

We are grateful to ECMWF for making their Interim reanalysis fields available. The fields used to compute the amplitudes and phases of the planetary waves are available from ECMWF (www.ecmwf.int). This work forms part of the Polar Science for Planet Earth programme of the British Antarctic Survey.

REFERENCES

Baines, P. G. and Fraedrich, K. 1989. Topographic effects on the mean tropospheric flow patterns around Antarctica. *Journal of the Atmospheric Sciences* **46**: 3401-3415.

Bals-Elsholz, T. M., Atallah, E. H., Bosart, L. F., Wasula, T. A., Cempa, M. J. and Lupo, A. R. 2001. The wintertime Southern Hemisphere split jet: Structure, variability, and evolution. *Journal of Climate* **14**: 4191-4215.

Bracegirdle, T. J. and Marshall, G. J. 2012. The reliability of Antarctic tropospheric pressure and temperature in the latest global reanalyses. *Journal of Climate* **25**: 7138-7146.

Dee, D. P., Uppala, S. M., Simmons, A. J., Berrisford, P., Poli, P., Kobayashi, S., Andrae, U., Balmaseda, M. A., Balsamo, G., Bauer, P., Bechtold, P., Beljaars, A. C. M., Van de Berg, L., Bidlot, J., Bormann, N., Delsol, C., Dragani, R., Fuentes, M., Geer, A. J., Haimberger, L., Healy, S. B., Hersbach, H., Holm, E. V., Isaksen, L., Kallberg, P., Kohler, M., Matricardi, M., McNally, A. P., Monge-Sanz, B. M., Morcrette, J. J., Park, B. K., Peubey, C., de Rosnay, P., Tavolato, C., Thepaut, J. N. and Vitart, F. 2011. The ERA-Interim reanalysis: configuration and performance of the data assimilation system. *Quarterly Journal of the Royal Meteorological Society* **137** [656]: 553-597.

Ding, Q. H., Steig, E. J., Battisti, D. S. and Wallace, J. M. 2012. Influence of the Tropics on the Southern Annular Mode. *Journal of Climate* **25** [18]: 6330-6348.

Fogt, R. L. and Zbacnik, E. A. 2014. Sensitivity of the Amundsen Sea Low to Stratospheric Ozone Depletion. *Journal of Climate* **27** [24]: 9383-9400.

Freitas, A. C. V. and Rao, V. B. 2014. Global changes in propagation of stationary waves in a warming scenario. *Quarterly Journal of the Royal Meteorological Society* **140** [679]: 364-383.

Garreaud, R. D. and Battisti, D. S. 1999. Interannual (ENSO) and interdecadal (ENSO-like) variability in the Southern Hemisphere tropospheric circulation. *Journal of Climate* **12**: 2113-2123.

Harangozo, S. A. 2000. A search for ENSO teleconnections in the west Antarctic Peninsula climate in Austral winter. *International Journal of Climatology* **20**: 663-679.

Hobbs, W. R. and Raphael, M. N. 2007. A representative time-series for the Southern Hemisphere zonal wave 1. *Geophysical Research Letters* **34** [5]: L05702, doi:10.1029/2006gl028740.

Holland, P. R. and Kwok, R. 2012. Wind-driven trends in Antarctic sea-ice drift. *Nature Geoscience* **5** [12]: 872-875.

Hosking, J. S., Orr, A., Marshall, G. J., Turner, J. and Phillips, T. 2013. The influence of the Amundsen-Bellingshausen Seas Low on the climate of West Antarctica and its representation in coupled climate model simulations. *Journal of Climate* **26**: 6633-6648.

Hoskins, B. J. and Karoly, D. J. 1981. The steady linear response of a spherical atmosphere to thermal and orographic forcing. *Journal of the Atmospheric Sciences* **38**: 1179-1196.

Houseago-Stokes, R. E. and McGregor, G. R. 2000. Spatial and temporal patterns linking southern low and high latitudes during South Pacific warm and cold events. *International Journal of Climatology* **20**: 793-801.

Irving, D. and Simmonds, I. 2015. A Novel Approach to Diagnosing Southern Hemisphere Planetary Wave Activity and Its Influence on Regional Climate Variability. *Journal of Climate* **28** [23]: 9041-9057.

Irving, D. and Simmonds, I. 2016. A new method for identifying the Pacific-South American pattern and its influence on regional climate variability. Journal of Climate : doi:10.1175/JCLI-D-15-0843.1.

Jin, D. and Kirtman, B. P. 2009. Why the Southern Hemisphere ENSO responses lead ENSO. *Journal of Geophysical Research-Atmospheres* **114** [D23101, doi: 10.1029/2009jd012657].

Jin, D. H. and Kirtman, B. P. 2010. The extratropical sensitivity to the meridional extent of tropical ENSO forcing. *Climate Dynamics* **34** [7-8]: 935-951.

Karoly, D. J. 1989. Southern Hemisphere circulation features associated with El Niño-Southern Oscillation events. *Journal of Climate* **2**: 1239-1252.

Kidson, J. W. 1999. Principal modes of Southern Hemisphere low-frequency variability obtained from NCEP-NCAR reanalyses. *Journal of Climate* **12** [9]: 2808-2830.

Kiladis, G. N. and Mo, K. C. 1998. Interannual and intraseasonal variability in the Southern Hemisphere. Karoly, D. J. and Vincent, D. G. Meteorology of the Southern Hemisphere. 307-336. American Meteorological Society.

Li, X., Gerber, E. P., Holland, D. M. and Yoo, C. 2015. A Rossby Wave Bridge from the Tropical Atlantic to West Antartica. *Journal of Climate* **28**: 2256-2273.

Li, X. C., Holland, D. M., Gerber, E. P. and Yoo, C. 2014. Impacts of the north and tropical Atlantic Ocean on the Antarctic Peninsula and sea ice. *Nature* **505** [7484]: 538-542 (doi: 10.1038/nature12945).

Liu, Z. Y. and Alexander, M. 2007. Atmospheric bridge, oceanic tunnel, and global climatic teleconnections. *Reviews of Geophysics* **45** [2]: RG2005, doi:10.1029/2005rg000172.

Mo, K. C. and Higgins, R. W. 1998. The Pacific-South American modes and tropical convection during the Southern Hemisphere winter. *Monthly Weather Review* **126** [6]: 1581-1596.

Pezza, A. B., Rashid, H. A. and Simmonds, I. 2012. Climate links and recent extremes in antarctic sea ice, high-latitude cyclones, Southern Annular Mode and ENSO. *Climate Dynamics* **38** [1-2]: 57-73.

Raphael, M. N. 2004. A zonal wave 3 index for the Southern Hemisphere. *Geophysical Research Letters* **31**: L23212, doi:10.1029/2004GL020365.

Raphael, M. N. 2007. The influence of atmospheric zonal wave three on Antarctic sea ice variability. *Journal of Geophysical Research* **112**: D12112, doi:10.1029/2006JD007852.

Raphael, M. N., Marshall, G. J., Turner, J., Fogt, R. L., Schneider, D. P., Dixon, D. A., Hosking, J. S., Jones, J. M. and Hobbs, W. R. 2016. The Amundsen Sea Low: Variability, change and impact on Antarctic Climate. *Bulletin of the American Meteorological Society*,97, 111-121, doi:10.1175/BAMS-D-14-00018.1.

Renwick, J. A. 2005. Persistent positive anomalies in the Southern Hemisphere circulation. *Monthly Weather Review* **133** [4]: 977-988.

Renwick, J. A. and Revell, M. J. 1999. Blocking over the South Pacific and Rossby wave propagation. *Monthly Weather Review* **127**: 2233-2247.

Schneider, D. P., Deser, C. and Okumura, Y. 2012. An assessment and interpretation of the observed warming of West Antarctica in the austral spring. *Climate Dynamics* **38** [1-2]: 323-347.

Simmonds, I. 2003. Modes of atmospheric variability over the Southern Ocean. *Journal of Geophysical Research - Oceans* **108** [C4]: doi:10.1029/2000JC000542.

Simpkins, G. R., McGregor, S., Taschetto, A. S., Ciasto, L. M. and England, M. H. 2014. Tropical Connections to Climatic Change in the Extratropical Southern Hemisphere: The Role of Atlantic SST Trends. *Journal of Climate* **27** [13]: 4923-4936.

Thompson, D. W. J., Solomon, S., Kushner, P. J., England, M. H., Grise, K. M. and Karoly, D. J. 2011. Signatures of the Antarctic ozone hole in Southern Hemisphere surface climate change. *Nature Geoscience* **4** [11]: 741-749.

Trenberth, K. E. 1980. Planetary waves at 500 mb in the southern hemisphere. *Monthly Weather Review* **108**: 1378-1389.

Trenberth, K. E., Fasullo, J. T., Branstator, G. and Phillips, A. S. 2014. Seasonal aspects of the recent pause in surface warming. *Nature Climate Change* **4** [10]: 911-916.

Trenberth, K. E. and Mo, K. C. 1985. Blocking in the Southern Hemisphere. *Monthly Weather Review* **113**: 3-21.

Turner, J. 2004. The El Niño-Southern Oscillation and Antarctica. *International Journal of Climatology* **24**: 1-31.

Turner, J., Bromwich, D., Colwell, S., Dixon, S., Gibson, T., Hart, T., Heinemann, G., Hutchinson, H., Jacka, K., Leonard, S., Lieder, M., Marsh, L., Pendlebury, S., Phillpot, H., Pook, M. and Simmonds, I. 1996. The Antarctic First Regional Observing Study of the Troposphere (FROST) project. Bulletin of the American Meteorological Society 77: 2007-2032.

Turner, J., Colwell, S. R. and Harangozo, S. A. 1997. Variability of precipitation over the coastal western Antarctic Peninsula from synoptic observations. *Journal of Geophysical Research* **102**: 13999-14007.

Turner, J., Colwell, S. R., Marshall, G. J., Lachlan-Cope, T. A., Carleton, A. M., Jones, P. D., Lagun, V., Reid, P. A. and Iagovkina, S. 2005. Antarctic climate change during the last 50 years. *International Journal of Climatology* **25**: 279-294.

Turner, J., Hosking, J. S., Marshall, G. J., Phillips, T. and Bracegirdle, T. J. 2016. Antarctic sea ice increase consistent with intrinsic variability of the Amundsen Sea Low. *Climate Dynamics*, 46, 2391-2402, DOI: 10.1007/s00382-015-2708-9.

Turner, J., Hosking, J. S., Bracegirdle, T. J., Marshall, G. J. and Phillips, T. 2015. Recent changes in Antarctic sea ice. *Philosophical Transactions of the Royal Society of London, Series A* **373**,20140163, doi:10.1098/rsta.2014.0163.

Van den Broeke, M. R. 1998. The semi-annual oscillation and Antarctic climate. Part 2: recent changes. *Antarctic Science* **10**: 184-191.

van Loon, H. 1979. The association between latitudinal temperature gradient and eddy transport. Part I: Transport of sensible heat in winter. *Monthly Weather Review* **107**: 525-534.

van Loon, H. and Jenne, R. 1972. The zonal harmonic standing waves in the Southern Hemisphere. *Journal of Geophysical Research* **77**: 992-1003.

van Loon, H. and Williams, J. 1976. The connection between trends of mean temperature and circulation at the surface: Part I. Winter. *Monthly Weather Review* **104**: 365-380.

Vecchi, G. A. and Wittenberg, A. T. 2010. El Nino and our future climate: where do we stand? *Wiley Interdisciplinary Reviews-Climate Change* **1** [2]: 260-270.

Yuan, X. 2004. ENSO-related impacts on Antarctic sea ice: A synthesis of phenomenon and mechanisms. *Antarctic Science* **16**: 415-425.